An Integrated Preventive Operation Framework for Power Systems During Hurricanes

Yuanrui Sang, *Member, IEEE*, Jiayue Xue, Mostafa Sahraei-Ardakani, *Member, IEEE*, and Ge Ou

***Abstract*—Severe weather is the primary cause of power outages in the U.S. Despite the availability of weather forecast information, such data are not systematically integrated into operation models. This article proposes an integrated framework to convert weather forecast into appropriate information for preventive operation during hurricanes so that the power outages induced by hurricanes can be reduced. To achieve this goal, first, a structural model of the transmission towers is developed to estimate failure probabilities based on the wind speed. These probabilities are then integrated within a day-ahead security-constrained unit commitment framework to guide preventive operation. The resulting day-ahead schedule will be more reliable as it will rely less on the elements that are likely to fail. Simulation studies, conducted on the IEEE 118-bus system affected by synthesized Irma and Harvey hurricanes, showed that the proposed framework was able to prevent 33% to 83% of the blackouts. Further research is required to investigate the impacts of flooding, damage to the distribution network, and weather forecast uncertainty.**

***Index Terms*—Dynamic structural modeling, extreme events, hurricane, power outage, power system reliability, power system resilience, preventive operation, stochastic optimization, transmission outage.**

NOMENCLATURE

A. Structural Model

Indices

l	Coefficient compared with limit state.
k	Transmission line.
i, j	Location indices of the transmission tower.
m	Indices of tower locations in the transmission line.

Variables

$F_R(V)$	Structural wind fragility at wind speed V.
$F_d(t)$	Wind load at time t.
V	Mean wind speed.
$V(t)$	Wind time history.
$V_g(r_g)$	Gradient wind speed at a radial distance of r_g from hurricane center.
$\bar{V}(z_i)$	Mean wind speed at height z_i.
r_g	Radial distance from hurricane center.
$F_R(V)$	Tower failure probability under wind speed *V*.
V_m	Mean wind speed at the mth tower location.
P_m	Damage and failure probability.
$P[FL, k]$	Failure probability of transmission line k.
$P[SL, k]$	Survival probability of transmission line k.

Parameters

A, B	Scaling factors for horizontal wind profile.
A_P	Projected area.
C_d	Drag coefficient.
f_c	Coriolis parameter.
p_n	Ambient pressure.
p_c	Central pressure.
V_{10}	Mean wind speed at height 10 m.
$\bar{V}$	Mean wind speed.
$\bar{V}_{10}$	10-min mean wind speed at the height of 10 m.
z	Height of mean wind speed.
z_{10}	Height constant of 10 m.
α	Ground roughness.
ρ	Air density.
NT	Number of towers in one transmission line.

B. Preventive Operation Model

Indices

k	Transmission line.
g	Generator.
n	Node.
s	Scenario.
seg	Segment of linearized generator cost function.

Sets

$\sigma^+(n)$	Transmission lines with their "to" bus connected to node n.
$\sigma^-(n)$	Transmission lines with their "from" bus connected to node n.
$g(n)$	Generators connected to node n.

Variables

$F_{k,s,t}$	Real power flow through transmission line k in scenario s at time t.
$L^L_{n,s,t}$	Load loss at node n in scenario s at time t.

Manuscript received March 28, 2019; revised August 25, 2019; accepted October 12, 2019. This work was supported in part by the NSF ECCS under Grant #1839833 and in part by the Utah Science Technology and Research Initiative under Grant #18065UTAG004. *(Corresponding author: Yuanrui Sang.)*

Y. Sang is with the Department of Electrical and Computer Engineering, The University of Texas at El Paso, El Paso, TX 79968 USA (e-mail: ysang@utep.edu).

J. Xue and G. Ou are with the Department of Civil and Environmental Engineering, The University of Utah, Salt Lake City, UT 84112 USA (e-mail: jiayue.xue@utah.edu; ge.ou@utah.edu).

M. Sahraei-Ardakani is with the Department of Electrical and Computer Engineering, The University of Utah, Salt Lake City, UT 84112 USA (e-mail: mostafa.ardakani@utah.edu).

Digital Object Identifier 10.1109/JSYST.2019.2947672

$P_{g,s,t}$	Real power generation of generator g in scenario s at time t.
$P^{O}_{g,s,t}$	Overgeneration of generator g in scenario s at time t.
$P^{\text{seg}}_{g,s,t}$	Real power generation of generator g in scenario$s$ in segment seg at time t.
$u_{g,t}$	Unit commitment (1: generator g is on at time t; 0: generator g is off at time t).
$v_{g,t}$	Startup variable (1: generator g starts up at time t; 0: generator g does not start up at time t).
$w_{g,t}$	Shutdown variable (1: generator g shuts down at time t; 0: generator g does not shut down at time t).
$\theta_{n,s,t}$	Voltage angle at bus n in scenario s at time t.
$\theta_{fr,\,k,s,t}$	Voltage angle at the "from" node of line k in scenario s at time t.
$\theta_{\text{to},k,s,t}$	Voltage angle at the "to" node of line k in scenario s at time t.

Parameters

b_k	Susceptance of transmission line k.
$c^{\text{linear}}_{g,\text{seg}}$	Linear cost of generator g in segment seg.
c^{L}	Cost of load loss ($/MWh).
c^{NL}_{g}	No-load cost of generator g.
c^{O}	Cost of over generation ($/MWh).
c^{SD}_{g}	Shutdown cost of generator g.
c^{SU}_{g}	Startup cost of generator g.
$F^{\max}_{k}$	Thermal/stability limit of transmission line k.
$L_{n,s,t}$	Load at bus n in scenario s at time t.
N_b	Number of buses in s system.
N_g	Total number of generators.
N_s	Number of scenarios.
N_{seg}	Number of segments for the linearized generator cost function.
p_{k,t_k}	Probability of line k to fail at time t_k.
p_s	Probability of scenario s.
$P^{\max}_{g}$	Upper generation limit of generator g.
$P^{\min}_{g}$	Lower generation limit of generator g.
$P^{\text{seg,max}}_{g}$	Upper generation limit of generator g in segment seg.
RR_g	Hourly ramp-rate for generator g.
t_H	The time that hurricane starts.
t_k	The time that line k fails.
T	Length of the investigated time period.
T_F	Number of periods with different probabilities of transmission line failure.
T^{down}_{g}	Minimum downtime for generator g.
T^{up}_{g}	Minimum uptime for generator g.
$z_{k,s,t}$	Transmission line k's status at time t in scenario s (1: line is closed; 0: line is open).
$\Delta\theta^{\max}_{k}$	Maximum value of bus voltage angle difference to maintain stability for line k.
$\Delta\theta^{\min}_{k}$	Minimum value of bus voltage angle difference to maintain stability for line k.

I. Introduction

ACCORDING to a report by the Department of Energy, severe weather is the leading cause of power outages in the U.S. [1]. Another report by six national laboratories warns that the frequency and intensity of weather-related hazards will continue to increase due to climate change [2]. The report also identifies four categories of resilience enhancement responses, which include robustness, resourcefulness, rapid recovery, and adaptability [2]. Hurricanes and tropical storms are one main category of extreme weather events that lead to large blackouts, both in terms of lost electric load and number of affected customers. The 2017 hurricane season clearly revealed the vulnerability of the U.S. electric power grid to the hurricanes. The impact of three major hurricanes that occurred in 2017 is summarized in Table I [3]–[8]. In August 2017, hurricane Harvey caused about 300 000 customer outages in Texas [4]. About two weeks later, in September, hurricane Irma led to the outage of more than six million customers in Florida (59% of total FL customers) [5] and just below a million customers in Georgia (22% of total GA customers) [6]. Later in September, Hurricane Maria made a devastating landfall in Puerto Rico, which left the entire island in complete darkness [7]. As of the end of 2017, more than three months after the hurricane's landfall, still, about 30% of the load was not recovered. Clearly, the existing reliability practices are inadequate during hurricanes.

Power system reliability is often achieved through the implementation of various redundancies so that the system withstands likely disturbances [9]–[11]. Reliability standards set by the North American Electric Reliability Corporation (NERC) require the operators to prevent blackouts under the random outage of one (*N*-1) or two (*N*-1-1) bulk power elements [12], [13]. Hurricanes, however, usually lead to an outage of multiple elements, well beyond the conditions of NERC standards. For example, Electric Reliability Council of Texas experienced 97 transmission line outages (139 kV and above) after hurricane Harvey made landfall [14]; similarly, hurricane Sandy caused the outage of over 218 high-voltage (115 kV and above) transmission lines [15]. Clearly, the conventional reliability tools, which the industry makes use of, are neither designed for nor applicable to such extreme conditions.

For the case of hurricanes, rich meteorological information, such as wind direction and speed, is forecasted and available to power system operators [15], [16]. Some system operators even have access to meteorologists onsite [15]. However, the weather information is often not converted to appropriate inputs for systematic use in preventive operation. The conservative changes to the operation procedures, during severe weather, is heavily based on engineering judgment and operators' knowledge. Thus, many effective but unknown preventive actions are missed, increasing the size of power outages.

A. Academic Literature

There is a vast body of academic literature that aims to estimate the power outage statistics (e.g., number of customers without power, etc.) with the weather forecast data before the hurricane [17]–[24]. Such statistical models, though may produce high-quality results, are only able to provide macroscale statistics about the outage, without any details on the element-level failures. There also exists a number of studies on system hardening and maintenance strategies considering weather

TABLE I
INFORMATION SUMMARY OF THREE MAJOR HURRICANES IN 2017

Hurricane Name	US landfall time	Landfall location	Customers affected	Transmission lines affected	Generators affected
Harvey	08/26/2017	Texas	0.3 million	339	1,168 MW wind power taken offline
Irma	09/10/2017	Florida	7 million	118	2 nuclear stations shutdown
Maria	09/20/2017	Puerto Rico	1.6 million (almost all customers in Puerto Rico)	NERC report not available yet	NERC report not available yet

conditions [25], [26] and optimizing the repair and restoration plan after the hurricane [27]–[32]. However, the literature on preventive operation during the hurricane, using weather forecast information, is almost nonexistent. Although there exists work on identifying power system vulnerability considering different contingencies [33], the knowledge of system vulnerability is not used in performing preventive operations. The only published research in the preventive operation domain that we are aware of includes [34], [35], and the authors' own study [36]–[38]. All these papers show promising prospect for preventive operation; however, they do not properly model the weather data, estimate the damage to power system components through dynamic structural analysis, and integrate the predicted damage information in day-ahead operation. A Sandia National Laboratory report [39], [40] briefly presents a method for modeling high-impact low-frequency events, which includes system fragility analysis, scenario generation, and system recovery. However, the report does not include mathematical models for system fragility and scenario generation and does not study the impacts of preventive operation. This article is the first to develop an integrated framework to study the effectiveness of preventive day-ahead operation during hurricanes, with detailed mathematical models for system fragility analysis, scenario generation, and power system preventive operation.

B. Industry Practices

Although the NERC reliability standards do not apply to the case of hurricanes, the utilities, as well as the state and federal governments, have taken steps to improve the resilience of the grid, under extreme weather conditions. The National Electrical Safety Code includes requirements for transmission and distribution lines of a certain height to be able to withstand strong winds, which is defined based on the region [41]. For instance, the T&D equipment in the coastal areas of Texas and Florida should withstand wind speeds of up to 130 mi/h [41]. It should be noted that the wind gust for both Harvey and Irma exceeded this threshold. Moreover, older transmission towers and distribution poles do not necessarily meet these standards.

The utility efforts can be divided into three categories: durability, resilience, and restoration [42]. Durability involves hardening efforts that would strengthen the system in the face of extreme conditions; resilience would enable the delivery of electricity despite some damage; and restoration reduces the outage time.

A number of utilities have made significant investments in hardening their T&D infrastructure. For example, Florida Power and Light (FPL) has spent $3 billion in undergrounding power lines, clearing vegetation in transmission corridors, strengthening power lines, inspecting poles, and replacing those that did not meet the standards [43]. Such efforts showed to be effective during Irma. Postmortem analysis of Maria has also led to suggestions on how to rebuild a more resilient system [44], [45]. FPL also invested significantly in smart grid technologies to monitor and automate the system [46]; however, an integrated framework that converts weather data into practical information for preventive operation is still needed.

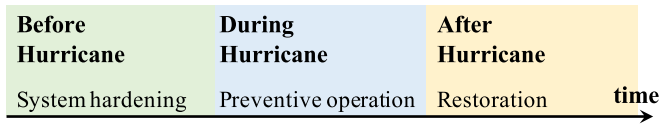

Fig. 1. Time window for the preventive operation model, developed in this article, compared to system hardening and restoration.

The utilities have also made progress in their restoration planning. Prepositioning of restoration crew and equipment, as well as seeking help from out of state utility and contractor workers are examples of such improvements [43], [47].

Despite the significant progress in system hardening and restoration, automated tools to improve the system resilience during a storm are nonexistent. Existing proactive actions are usually identified and executed based on engineering judgment. For instance, the utilities de-energized a number of substations in the New York City during Superstorm Sandy to prevent damage to their equipment [48]. These actions led to transmission overloads that resulted in additional power outages [48]. An NERC report lists the actions that were taken during hurricane Irma, which included increasing the staff, postponing scheduled outages for maintenance, and prestaging repair crew and equipment [8]. Lack of automated operator advisory tools, which motivates the this article, is apparent.

C. Scope of Contributions of This Article

This article investigates the potential benefits as well as the design principles of an operator advisory tool during hurricanes. The tool provides system operators with preventive actions with the goal of reducing power outages. This tool is designed during for the short-time window, covering a few days prior to hurricane landfall until the point when the storm is weakened and not of concern anymore. Therefore, the proposed model offers a fundamentally different functionality compared with system hardening or restoration efforts, as shown in Fig. 1.

As a first step, this article focuses on testing the viability of this framework. To enable the analysis, a number of simplifying

assumptions are made. The promising results presented later in this article suggest that the proposed framework has the potential of delivering sizeable reliability improvements. Further research is required to better understand the performance of the proposed framework under a more realistic set of assumptions. The main simplifying assumptions are briefly discussed ahead.

First, this article exclusively focuses on transmission-level component damages. Historic data verify that generators are usually not prone to damage by hurricanes, as they are protected in an indoor environment with strong structural support [49]. The exception to this is flooding, which may cause generation outage. This article at hand, however, focuses on extreme wind impacts rather than modeling the impacts of other types of extreme weather, such as flooding. Therefore, in the analysis offered in this article, direct generator outage is not considered. However, the proposed framework can be seamlessly extended to allow for modeling of generation outages by adding additional scenarios. In addition to direct outage of generation, loss of transmission lines may lead to disconnected generators. In such cases, the power produced by the disconnected generator will not be deliverable to the load. This type of generator outage is considered in this article and modeled through overgeneration variables, which similar to the lost load, is penalized with a high penalty factor in the objective function. The same report confirms that hurricanes cause significant damage to T&D systems [49]. Due to the radial arrangement of the distribution network, there is very little room for preventive operation at the distribution level. Thus, we acknowledge the vulnerability of the distribution network to severe weather, but choose to overlook it in this article. To further justify this assumption, it is important to note that power outages caused by distribution-level damages are local. However, transmission-level failures can lead to power outages far outside the area directly affected by the hurricane, where the distribution network is not affected. Such outages are likely avoidable through the model developed in this article.

Second, this article exclusively focuses on the wind feature of the hurricanes, ignoring other factors such as flooding. Again, we acknowledge that flooding may damage the power system components. However, the majority of the failures during a hurricane is caused by its strong winds. Third, in the structural modeling, only the structural buckling and collapse of the transmission tower is considered, which can be further expanded to including conductor breaking, transmission wire damage, and even debris impact. Lastly, the weather forecast information includes inherent uncertainties [50]; however, to simplify the study, this article assumes that the weather forecast is exact.

The preventive operation framework proposed in this article includes three modules, as shown in Fig. 2. First, weather forecast information is employed to estimate the damages to transmission system components. To do so, a structural model is developed, which analyzes the failure of transmission towers, due to the dynamic wind loading. The model estimates the likelihood of transmission line failure as a function of wind speed. Second, contingency scenarios are generated considering the combinations of component failures at different times. At last, the contingency scenarios are adopted in the stochastic day-ahead security-constrained unit commitment (SCUC). Load

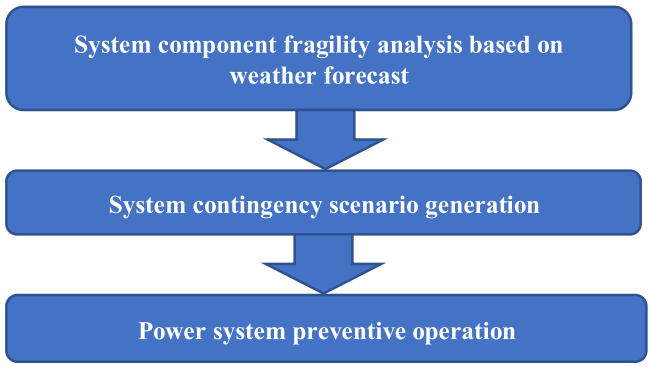

Fig. 2. Illustration of the preventive operation framework.

shedding and overgeneration are penalized with high penalty factors in the SCUC formulation. Thus, the electric load will only be shed if the damaged network cannot support the delivery of energy to a location, or if such delivery is extremely costly. The mathematical representation of this problem is a stochastic mixed-integer linear program. To reduce the computational burden of the problem, a simple scenario reduction technique is used. The schedule, obtained by this framework, will rely less on the transmission elements that are prone to failure due to the hurricane. Thus, the system reliability will be enhanced and the power outage will be reduced.

The proposed preventive operation model is based on dc power flow, since currently all the power system operators in the U.S. use dc-power-flow-based optimization models for operation. The model enforces a number of hard constraints, including the transmission line thermal limits, which ensure that no transmission line is overloaded under any scenario. Voltage stability is beyond the scope of this study and will be addressed in future work.

The simulation results, presented in this article, suggest that appropriate integration of weather data in power system operation will significantly reduce power outages during hurricanes. This reduction in our simulation studies, for the IEEE 118-bus system under synthesized Irma and Harvey hurricane scenarios, was between 33% and 83%, which is rather encouraging.

The rest of this article is organized as follows. Section II presents the transmission tower structural model and its stability under dynamic wind loading. Section III describes the generation of contingency scenarios, using the failure probabilities, estimated through the structural model. Section IV develops the preventive SCUC model using the stochastic optimization. Case studies are presented and discussed in Section V. A brief discussion of the computational complexity of the model is presented in Section VI and, finally, Section VII concludes this article.

II. Transmission Tower Dynamic Response Under Wind Loading

This section briefly explains the derivation of a finite-element model of transmission towers to enable fragility analysis. All the towers are assumed to follow a generic design [51], which is

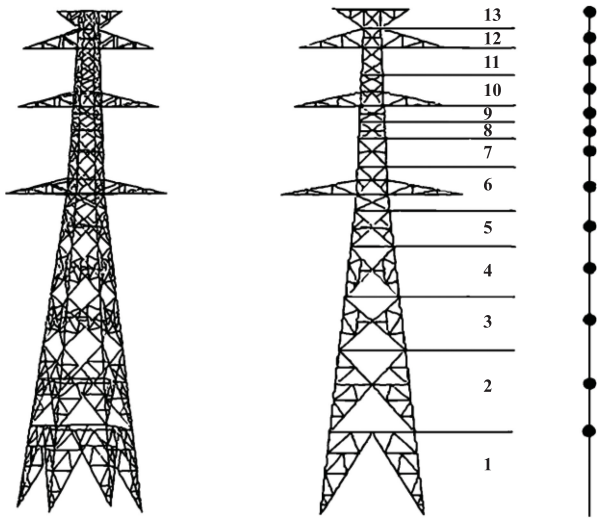

Fig. 3. Finite-element model and a simplified model of transmission towers.

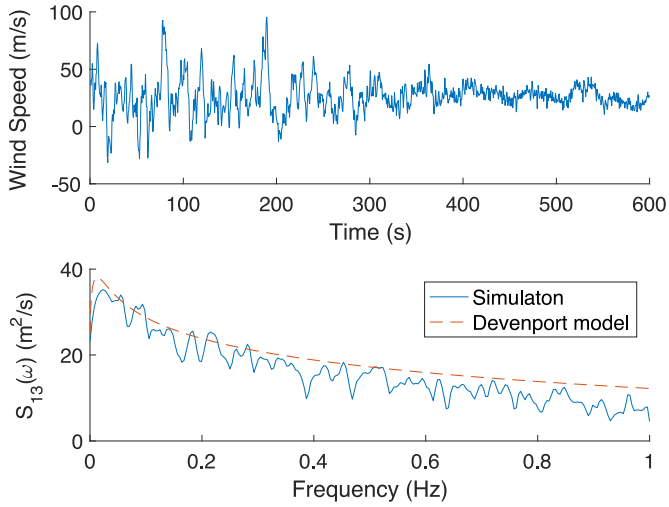

Fig. 4. Wind time history and validation. Top: wind speed at the tower tip. Bottom: comparison between simulated and theoretical value.

another simplifying assumption, with a height of 55 m, steel-made members, and L-shaped cross sections. A finite-element model of this tower is built in ANSYS. To reduce the computational time, the tower model is further reduced into a 13-degree-of-freedom-lumped mass model, as shown in Fig. 3.

Dynamic wind loading characteristics are composed of steady and fluctuating wind components [52]. For mean wind component, the changes over height are described by the power-law [53], as shown in (1). For most transmission towers that are built in the open plain, α equals 0.16

$$\frac{\bar{V}}{\bar{V}_{10}} = \left(\frac{z}{z_{10}}\right)^{\alpha}. \tag{1}$$

Fluctuating wind speed is simulated through the weighted amplitude wave superposition method. According to the wind speed record, fluctuating wind speed can be expressed as a Gaussian stationary random process [54]. Fluctuating wind component is simulated using the developed model. There are 13 wind speeds at different heights based on the division of the transmission tower. The fluctuating wind speed at the top of the tower is shown in Fig. 4 (top); this wind speed is then compared with the desired power spectrum, as shown in Fig. 4 (bottom).

Dynamic wind loading is derived from wind time history and projected area [55], shown as follows:

$$F_d(t) = 0.5\rho V(t)^2 C_d A_P \tag{2}$$

where air density ρ is chosen as 1.195 kg/m^3. $V(t)$ is the wind time history, which is the sum of the mean wind and fluctuating wind components. Drag coefficient C_d is usually determined by the wind tunnel test [55]. In this article, we assume that all wind loads are added on the transmission tower perpendicularly. Thus, we choose the drag coefficient based on the literature with similar transmission tower shape and height [55], [56]. By adding wind load on the finite-element model and simplified lumped mass model, the top tip displacement of the transmission tower is demonstrated in Fig. 5.

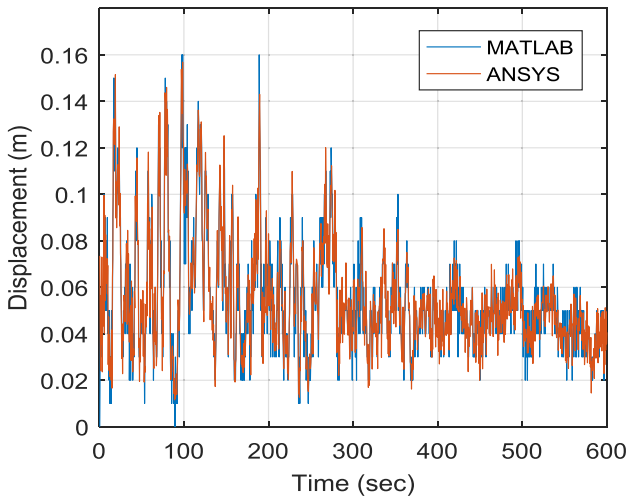

Fig. 5. Comparison of the top displacement between finite element and lumped mass models.

A. *Transmission Tower Fragility Under Extreme Wind*

A fragility curve describes the likelihood of damage and failure of a structure under different loading intensities, such as earthquake ground motion [57] or wind speed. In structural wind fragility, the damage and failure probability $F_R(V)$ under a given wind speed V can be calculated as

$$F_R(V) = P[l > \mathrm{LS}/V_{10} = V]. \tag{3}$$

The damage condition is defined as the structure performance exceeding a limit state (LS). In this article, the limit states are determined as transmission tower's top displacement over tower height at 1.5%, 2%, 2.5%, and 3%. Different fragility curves under different limit states are demonstrated in Fig. 6. The marked points are the probability of damage or failure of the individual tower under different wind speeds. The solid curve is the fitted normal cumulative distribution function. In this article,

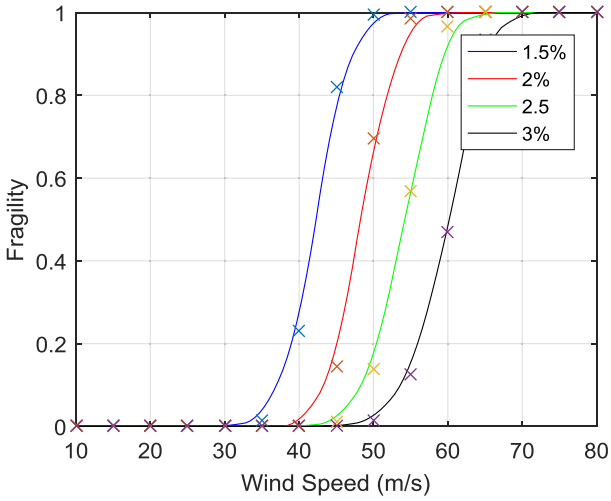

Fig. 6. Wind fragility curve of a transmission tower.

the failure condition of all transmission towers is determined at a displacement of over 2.5%.

B. Transmission System Fragility Under Extreme Wind

In order to estimate the performance of the transmission system in the hurricane region, two steps of calculation are involved. First, a horizontal wind profile is required to model the wind speed distribution in the region, affected by the hurricane. The horizontal wind profile can be expressed via [58]

$$V_g(r_g) = \left[\frac{AB(p_n - p_c)\exp\left(-\frac{A}{{r_g}^B}\right)}{\rho {r_g}^B} + \frac{{r_g}^2 {f_c}^2}{4} \right]^{1/2} - r_g f_c/2 \tag{4}$$

where $V_g(r_g)$ is the gradient wind speed as a function of radial distance r_g from the center of the hurricane. Wind speed increases linearly within the 100-km range of the hurricane center; outside that range, wind speed shows a parabolic attenuation.

The second step requires the calculation of each transmission line's failure probability based on the mth individual transmission tower's failure probability $P_m = F_{R,m}(V_m)$. We denote the kth transmission line's failure probability by $P[FL,k]$, and its survival probability by $P[SL,k]$. For a transmission line to survive a wind load, all of its towers must survive. Thus, $P[FL,k]$ can be calculated as

$$P[FL,k] = 1 - P[SL,k] = 1 - \prod_{m=1}^{NT} F_{R,m}(V_m). \tag{5}$$

According to the horizontal wind profile and hurricane movement track, wind speed at each tower location at each time interval can be estimated, which is, then, used to calculate the failure probability of the line.

III. Transmission Outage Scenario Generation

Based on the likelihood of each transmission failure, contingency scenarios can be generated and their probabilities are also calculated. Since different lines may fail at different times during the hurricane, each scenario should indicate the lines that fail and the time when each of those lines goes out of service. The scenario generation procedure is illustrated in Fig. 7.

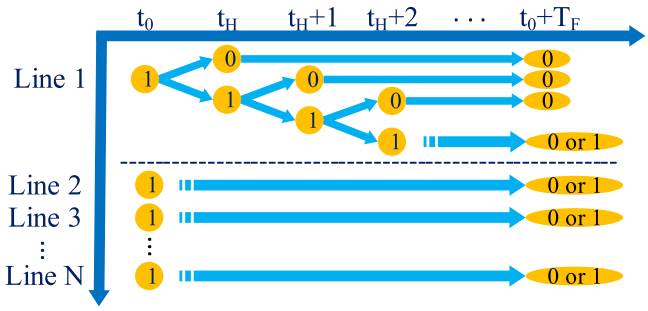

Fig. 7. Illustration of the scenario generation procedure.

According to Fig. 7, each scenario can be uniquely identified by a vector with N_{br} components, each of which indicating the time of failure for a particular line. If a line remains in service in a given scenario, the respective value for the line in the scenario vector should be greater than the time range of the study, i.e., $t_0 + T_F + 1$, which means that the line does not fail within the duration of the SCUC. The total number of scenarios can, thus, calculated as

$$N_s = (T_F + 1)^{N_{br}}. \tag{6}$$

Given that transmission line k fails at t_k in scenario s, the probability for each scenario is calculated as

$$p_s = \prod_{k=1}^{N_{br}} \left(p_{k,t_k} \prod_{t=t_H}^{t_k - 1} (1 - p_{k,t}) \right). \tag{7}$$

Equation (6) clearly shows how the number of scenarios can grow very quickly as the number of lines that are affected increases. The size of the scenario set greatly impacts the computational time, required for solving the optimization problem. Thus, it is essential to reduce the scenario size to an acceptable level. In this article, we use a very simple method and filter out the scenarios that have a probability below a cutoff level.

IV. Preventive Stochastic Optimization Model

The proposed preventive stochastic optimization model is based on a dc SCUC formulation where transmission outage scenarios, caused by the hurricane, are explicitly modeled. The problem identifies a single unit commitment solution for all the scenarios while allowing generation dispatch to vary for each scenario, within the ramping limits. Both overgeneration and load shedding are allowed under the scenarios but penalized with a high penalty price in the objective function.

The objective function is expressed in (8), which minimizes the expected dispatch cost of the system considering generation dispatch, overgeneration, and load shedding under all scenarios. Generation limits are expressed in (9)–(11); generation costs are calculated using a piecewise linear cost function. DC power flow constraints are expressed in (12) and (13); when a transmission

line is out of service, both its susceptance and capacity limit are set to 0 using the binary integer parameter $z_{k,s,t}$. Equation (14) sets the voltage angle of the reference bus to 0. Equation (15) is the nodal power balance constraint in which overgeneration and load shedding are included. Equations (16) and (17) calculate the start-up and shut-down variables; eq. (18) is the hourly ramping limit for each generator; eqs. (19) and (20) are the minimum up and downtime constraints for each generator. Since the contingencies are explicitly modeled, reserve requirements are omitted

$$\min\left(\sum_{s=1}^{N_s} p_s \sum_{t=1}^{T}\left(\begin{array}{c}\sum_{g=1}^{N_g}\left(\begin{array}{c}\sum_{\text{seg}=1}^{N_{\text{seg}}} c_{g,\text{seg}}^{\text{linear}} P_{g,s,t}^{\text{seg}} + c_g^{NL} u_{g,t} \\ + c_g^{SU} v_{g,t} + c_g^{SD} w_{g,t} + c^O P_{g,s,t}^O\end{array}\right) \\ + \sum_{n=1}^{N_b} c^L L_{n,s,t}^L\end{array}\right)\right) \tag{8}$$

$$P_{g,s,t} = \sum_{\text{seg}=1}^{N_{\text{seg}}} P_{g,s,t}^{\text{seg}} \tag{9}$$

$$0 \le P_{g,s,t}^{\text{seg}} \le P_g^{\text{seg,max}} \tag{10}$$

$$u_{g,t} P_g^{\min} \le P_{g,s,t} \le u_{g,t} P_g^{\max} \tag{11}$$

$$-z_{k,s,t} F_k^{\max} \le F_{k,s,t} \le z_{k,s,t} F_k^{\max} \tag{12}$$

$$z_{k,s,t} b_k \left(\theta_{fr,k,s,t} - \theta_{to,k,s,t}\right) = F_{k,s,t} \tag{13}$$

$$\theta_{1,s,t} = 0 \tag{14}$$

$$\sum_{k\in\sigma^+(n)} F_{k,s,t} - \sum_{k\in\sigma^-(n)} F_{k,s,t} + \sum_{g\in g(n)} P_{g,s,t} - P_{g,s,t}^O = L_{n,s.t} - L_{n,s,t}^L \tag{15}$$

$$v_{g,t} - w_{g,t} = u_{g,t} - u_{g,t-1} \tag{16}$$

$$v_{g,t} + w_{g,t} \le 1 \tag{17}$$

$$-\text{RR}_g \le P_{g,s,t} - P_{g,s,t-1} \le \text{RR}_g \tag{18}$$

$$\sum_{t=m}^{m+T_g^{\text{up}}-1} u_{g,t} \ge T_g^{\text{up}} \left(u_{g,m} - u_{g,m-1}\right)$$

$$2 \le m \le T - T_g^{\text{up}} + 1 \tag{19}$$

$$\sum_{t=m}^{m+T_g^{\text{down}}-1} \left(1 - u_{g,t}\right) \ge T_g^{\text{down}} \left(u_{g,m-1} - u_{g,m}\right)$$

$$2 \le m \le T - T_g^{\text{down}} + 1. \tag{20}$$

V. Simulation Studies

This section studies the effectiveness of the developed model through simulation on the IEEE 118-bus system [59]. To provide a better understanding, two separate cases are built, where the hurricanes affect different parts of the system. First, we mapped the IEEE 118-bus system to the transmission network in Texas. The first case includes 13 buses from IEEE 118-bus and 19 transmission lines as shown in Fig. 8 (left), denoted as layout I. The second case includes 20 buses and 23 lines as shown in Fig. 8 (right), denoted as layout II. Two hurricane scenarios were also generated, synthesizing Hurricanes Harvey and Irma. In both scenarios, the maximum sustained wind speed is extracted from the National Hurricane Center database [60]. Fig. 9 (top) shows hurricane Harvey's peak wind speed from 4 A.M. August 26th to 4 A.M. August 27th and Fig. 9 (bottom) shows hurricane Irma's peak wind speed from 5 P.M. September 9th to 5 P.M. September 10th. According to Section II, horizontal wind speed profile can be approximated, as shown in Fig. 10.

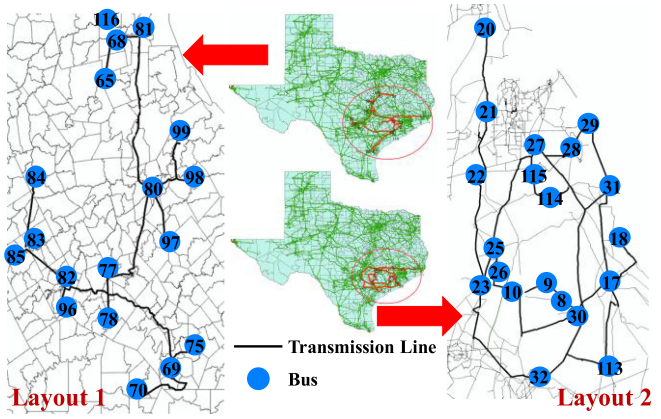

Fig. 8. Two mappings of the IEEE 118-bus system on Texas transmission grid.

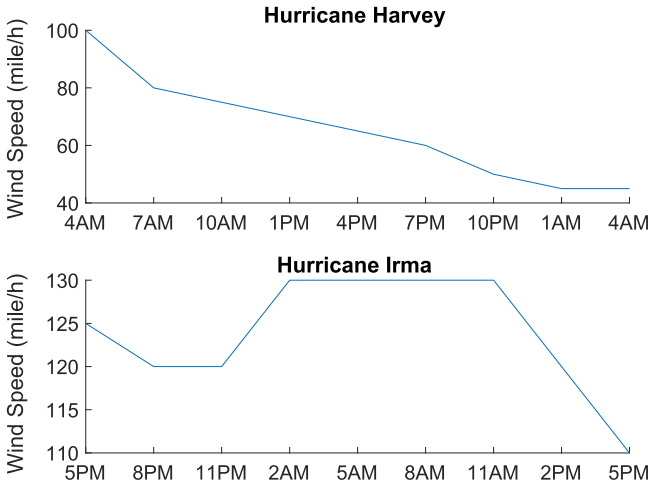

Fig. 9. Peak wind speed of hurricanes Harvey and Irma for 24 h.

A. Transmission System Fragility Analysis

According to the transmission system analysis procedure, described in Section II, failure probabilities of the transmission lines under synthesized hurricanes Harvey and Irma can be estimated. The accumulated probabilities at different time intervals are provided in Tables II–IV.

B. Transmission Outage Scenarios

Using the information provided in Tables II–IV, all the possible transmission outage scenarios were generated for the four cases (two hurricanes passing through two different parts of the

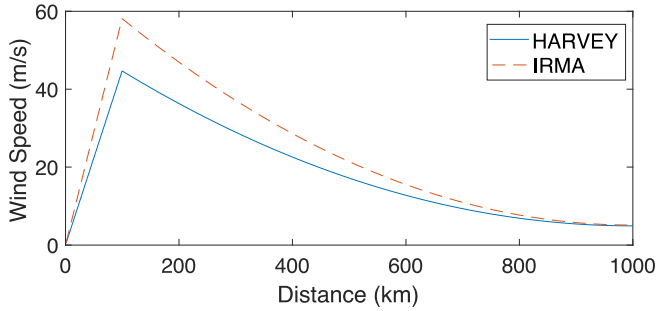

Fig. 10. Horizontal wind profile as a function of radius distance.

TABLE II
TRANSMISSION LINE FAILURE PROBABILITIES UNDER HARVEY

Harvey I			**Harvey II**		
Line number	4AM	7AM – 4AM	Line number	4AM	7AM-4AM
69-70	0	0	10-9	0.95	0.95
69-75	0	0	9-8	0.96	0.96
69-77	0	0	8-30	0.49	0.49
78-77	0	0	30-17	0.74	0.74
82-77	0	0	17-18	0.96	0.96
82-96	0	0	17-113	0.55	0.55
82-83	0	0	113-32	0	0
85-83	0	0	32-31	0.96	0.96
84-83	0	0	29-31	0.99	0.99
77-80	0.63	0.63	28-29	0.99	0.99
97-80	0.83	0.83	27-28	0.99	0.99
98-80	0.96	0.96	27-115	0.99	0.99
99-80	0.99	0.99	114-115	0.99	0.99
80-79	0.96	0.96	114-32	0.98	0.98
80-81	0.99	0.99	27-32	0.99	0.99
65-68	0.95	0.95	27-25	1	1
68-116	0.99	0.99	26-25	0.60	0.60
66-65	0.16	0.15	23-25	0.42	0.42
69-68	0.93	0.93	23-32	0.14	0.14
			23-22	0.88	0.88
			21-22	0.94	0.94
			20-21	0.89	0.89
			26-30	0.51	0.51

TABLE III
TRANSMISSION LINE FAILURE PROBABILITIES UNDER IRMA I

Line number	**5PM**	**8PM**	**11PM**	**2AM**	**5AM**	**8AM -5PM**
69-70	0	0	0	0.99	1	1
69-75	0	0	0.33	1	1	1
69-77	0.01	0.86	1	1	1	1
78-77	0	0.42	1	1	1	1
82-77	0	0.65	1	1	1	1
82-96	0	0.01	0.98	1	1	1
82-83	0	0.20	1	1	1	1
85-83	0	0.01	0.91	1	1	1
84-83	0.09	0.55	1	1	1	1
77-80	1	1	1	1	1	1
97-80	1	1	1	1	1	1
98-80	1	1	1	1	1	1
99-80	1	1	1	1	1	1
80-79	1	1	1	1	1	1
80-81	1	1	1	1	1	1
65-68	1	1	1	1	1	1
68-116	1	1	1	1	1	1
66-65	0.78	1	1	1	1	1
69-68	1	1	1	1	1	1

TABLE IV
TRANSMISSION LINE FAILURE PROBABILITIES UNDER IRMA II

Line number	**5PM**	**8 PM and later**	**Line number**	**5PM**	**8 PM and later**
10-9	1	1	114-115	1	1
9-8	1	1	114-32	1	1
8-30	1	1	27-32	1	1
30-17	1	1	27-25	1	1
17-18	1	1	26-25	1	1
17-113	1	1	23-25	1	1
113-32	0.11	1	23-32	1	1
32-31	1	1	23-22	1	1
29-31	1	1	21-22	1	1
28-29	1	1	20-21	1	1
27-28	1	1	26-30	1	1
27-115	1	1			

TABLE V
NUMBER OF SCENARIOS CONSIDERED IN EACH CASE

Hurricane cases	Harvey I	Harvey II	Irma I	Irma II
Number of scenarios	40	157	134	2

system). Each scenario is a vector, including information about the status of all the transmission lines at each hour in the studied period. In order to reduce the computational burden, scenarios with a probability of less than 0.1% were eliminated. The probabilities of the remaining scenarios were adjusted proportionally so that they sum up to 1. The number of simulated scenarios for each case is shown in Table V.

C. Preventive Operation

Hurricane Harvey made landfall around 4:00 A.M., and it was able to cause transmission line failures only in the first three hours, so the uncertainty of transmission line failures caused by this hurricane exists only on the day that the hurricane made its landfall. However, for the case of hurricane Irma, it made its landfall around 5:00 P.M., and was able to cause transmission line failures over the next 15 hours. Thus, the uncertainty of damage lasts into two days. In order to study the impact of the two hurricanes in a sufficiently long period, while considering the industrial practices for operating a day-ahead market, the impact of hurricane Harvey was studied in a 24-h SCUC model, whereas that of the hurricane Irma was studied in a 48-h SCUC model. The simulations were carried out in the following manner.

1) Two deterministic SCUC models, without considering the outage scenarios, were carried out as base cases according to the base case formulation presented in [61], one over 24 h and the other over 48 h.
2) The unit commitment results were obtained from the two base cases and fixed in the stochastic model to calculate the expected load shedding and over-generation under the hurricane scenarios with business as usual (BAU) operation.
3) The SCUC was optimized using the stochastic model, in order to evaluate the impact of the hurricanes with the preventive SCUC model. Steps 2) and 3) were carried out for the four cases listed in Table V.

TABLE VI
EXPECTED COST COMPARISON ($M)

Hurricane case	Base case	BAU w/ penalties	Preventive model w/ penalties	BAU w/o penalties	Preventive model w/o penalties
Harvey I	1.14	57.09	33.97	1.01	1.11
Harvey II	(1 day)	160.48	32.96	1.15	1.72
Irma I	2.28	154.49	105.49	2.00	2.33
Irma II	(2 days)	388.35	66.83	2.17	3.10

TABLE VII
EXPECTED LOST LOAD AND OVERGENERATION

Hurricane case	BAU		Preventive operation	
	Expected lost load	Expected over-generation	Expected lost load	Expected over-generation
Harvey I	6.23%	0.00%	3.65%	0.00%
Harvey II	12.91%	4.79%	3.46%	0.01%
Irma I	8.47%	0.00%	5.73%	0.00%
Irma II	15.25%	6.20%	3.54%	0.00%

As both load shedding and overgeneration are undesirable, they were penalized with a penalty factor of $10 000/MWh in the stochastic model. The SCUC was formulated and coded in Java using the CPLEX Java API and solved using the CPLEX MILP solver.

The expected dispatch costs were obtained for the four cases under both BAU and the proposed preventive model and compared with the base cases in Table VI. The results are presented both including and excluding the penalties for overgeneration and load shedding. As the penalty price is very large, the cost is dominated by its penalty component, when penalties are included. In such cases, the preventive model shows an obvious advantage in terms of achieving a lower cost solution, as it effectively reduces overgeneration and load shedding. It is difficult to compare the costs when penalties are excluded because the cost will generally decrease as more load is shed. Thus, comparison purely based on cost is not very meaningful here. However, in three out of four cases, the stochastic preventive model converges to a higher cost solution both compared with the base case and BAU. The largest increase from the base case is for Harvey II, where the preventive model adds 51% to the cost. However, the additional cost will help significantly enhance the system reliability, as will be discussed later in Table VII.

The expected load shedding and overgeneration from the four cases, under BAU and preventive operation, were calculated as a percentage of the overall demand during the studied period and presented in Table VII. In all cases, the preventive model was able to reduce the violations anywhere between 33% and 83%. As the damages for layout II was especially significant, with the BAU model, not only did the load shedding double, but also there was a 4%–7% of overgeneration, which caused much larger penalty costs compared with layout I. Using the preventive SCUC model, overgeneration was practically eliminated, and the expected load shedding was reduced to much lower levels, even for the case of Irma II, with a stronger hurricane and a more vulnerable layout. Thus, the mediocre increase in costs, presented in Table VI, is essentially the cost of reliability enhancement, which was rather significant, as shown in Table VII.

TABLE VIII
SOLUTION TIME OF THE FOUR CASES

Hurricane case	Harvey I	Harvey II	Irma I	Irma II
Solution time (min)	46.63	494.51	2889.28	0.31

VI. COMPUTATIONAL COMPLEXITY

The optimization problem, developed in this article, is a stochastic mixed-integer linear program. Solution time in this class of problems is heavily influenced by the number of integer variables and scenarios. The solution times for the four cases, presented in this article, are shown in Table VIII. For instance, Harvey II and Irma I had a similar number of scenarios, but Irma I was solved over 48 h, whereas Harvey II was solved over 24 h. Thus, Irma I involved a larger number of variables, especially binary commitment variables. This made the solution time for Irma I significantly longer than Harvey II. Harvey I and Irma II had relatively small numbers of scenarios, and both of them were solved in a relatively short period of time.

It should be noted that the solution time can be substantially longer for larger systems. Solving unit commitment problem for a large-scale power system in and of itself is a computationally challenging problem, let alone considering all the possibilities related to hurricane impacts. In industry implementations of unit commitment, a variety of simplifications and modeling techniques are used to achieve tractability. These include the adoption of sensitivity factors, iterative selection of binding constraints, as well as effective selection and reduction of the scenarios. In addition, large systems can be divided into a number of zones, and the problem can be solved in multiple stages. The purpose of this article, however, is to introduce the integrated framework, its components, and the effectiveness of the proposed methodology. Detailed investigation of tractability issues will require further research and will be discussed in our future work.

VII. CONCLUSION

This article, for the first time, develops an integrated framework where weather forecast information is effectively incorporated in power system operation. First, a finite-element structural model of transmission towers is developed. The model takes weather data as an input and calculates the failure probability of the transmission lines. These probabilities are then explicitly included within a day-ahead unit commitment model. Thus, the integrated framework is able to guide effective preventive operation under extreme weather conditions. The proposed framework was validated against business as usual operation under Hurricanes Irma and Harvey, synthesized for IEEE 118-bus system. To explore the feasibility and effectiveness of preventive operation, incorporating weather information, the simulation studies assumed that the weather forecast is exact. The results suggest that the proposed integrated framework is able to drastically reduce

power outages (33%–83%), during hurricanes by moderately increasing the operation cost (up to 51%). Further research is required for improving the computational efficiency of the developed model and testing on real-world large-scale systems. Future research will also study the impacts of weather forecast uncertainty on the effectiveness of preventive operations.

REFERENCES

[1] The President's Council of Economic Advisers and US Dept. Energy, "Economic benefits of increasing electric Grid resilience to weather outages," White House Office Sci. Technol., Aug. 2013.

[2] B. L. Preston *et al.*, "Resilience of the U.S. electricity system: A multi-hazard perspective," US Dept. Energy, Washington, DC, USA, Aug. 2016.

[3] "Hurricane Harvey event analysis report," North Amer, Elect, Rel. Corp., Atlanta, GA, USA, Tech. Rep., Mar. 2018. [Online]. Available: https://www.nerc.com/pa/rrm/ea/Hurricane_Harvey_EAR_DL/NERC_Hurricane_Harvey_EAR_20180309.pdf

[4] US Dept. Energy, Washington, DC, USA, "Infrastructure security and energy restoration, Hurricane Harvey event report (update 4), 2017.

[5] US Dept. Energy, Washington, DC, USA, "Infrastructure security and energy restoration, Hurricane Irma and Hurricane Harvey event summary (report 26), 2017.

[6] US Dept. Energy, Washington, DC, USA, "Infrastructure security and energy restoration, Hurricane Irma and Hurricane Harvey event summary (report 28), 2017.

[7] US Dept. Energy, Washington, DC, USA, "Infrastructure security and energy restoration, Hurricanes Maria, Irma, and Harvey September 22 afternoon event summary (report 43), 2017.

[8] "Hurricane Irma event analysis report," North Amer. Elect, Rel. Corp., Atlanta, GA, USA, Tech. Rep., Aug. 2018. [Online]. Available: https://www.nerc.com/pa/rrm/ea/Hurricane_Irma_EAR_DL/September%202017%20Hurricane%20Irma%20Event%20Analysis%20Report.pdf

[9] A. Lisnianski, G. Levitin, H. Ben-Haim, and D. Elmakis, "Power system structure optimization subject to reliability constraints," *Elect. Power Syst. Res.*, vol. 39, no. 2, pp. 145–152, 1996.

[10] G. Levitin, A. Lisnianski, and D. Elmakis, "Structure optimization of power system with different redundant elements," *Elect. Power Syst. Res.*, vol. 43, no. 1, pp. 19–27, 1997.

[11] Z. Xie, G. Manimaran, V. Vittal, A. Phadke, and V. Centeno, "An information architecture for future power systems and its reliability analysis," *IEEE Trans. Power Syst.*, vol. 17, no. 3, pp. 857–863, Aug. 2002.

[12] Criteria for Reliability Coordinator Actions to Operate Within IROLs, NERC Standard IRO-008-1, North Amer. Elect. Rel. Corp., Atlanta, GA, USA, 2014.

[13] Criteria for Reliability Coordinator Actions to Operate Within IROLs, NERC Standard IRO-009-1, North Amer. Elect. Rel. Corp., Atlanta, GA, USA, 2014.

[14] *Testimony of Walt Baum—Executive Director Texas Public Power Association,* Resiliency: The Electric Grid's Only Hope. House Science, Space, and Technology Committee, Washington, DC, USA, 2017. [Online]. Available: https://science.house.gov/imo/media/doc/Baum%20Testimony.pdf

[15] "Hurricane Sandy event analysis report," North Amer. Elect. Rel. Corp., Atlanta, GA, USA, Tech. Rep., 2014.

[16] K. Zhou, C. Fu, and S. Yang, "Big data driven smart energy management: From big data to big insights," *Renew. Sustain. Energy Rev.*, vol. 56, pp. 215–225, 2016.

[17] D. Zhu, D. Cheng, R. P. Broadwater, and C. Scirbona, "Storm modeling for prediction of power distribution system outages," *Elect. Power Syst. Res.*, vol. 77, no. 8, pp. 973–979, 2007.

[18] R. Nateghi, S. Guikema, and S. M. Quiring, "Power outage estimation for tropical cyclones: Improved accuracy with simpler models," *Risk Anal.*, vol. 34, no. 6, pp. 1069–1078, 2014.

[19] H. Liu, R. A. Davidson, and T. V. Apanasovich, "Statistical forecasting of electric power restoration times in hurricanes and ice storms," *IEEE Trans. Power Syst.*, vol. 22, no. 4, pp. 2270–2279, Nov. 2007.

[20] S. R. Han, "Estimating hurricane outage and damage risk in power distribution systems," Ph.D. Diss., Dept. Civil Environ. Eng., Texas A&M University, College Station, TX, USA, 2008.

[21] S. D. Guikema, S. M. Quiring, and S.-R. Han, "Prestorm estimation of hurricane damage to electric power distribution systems," *Risk Anal.*, vol. 30, no. 12, pp. 1744–1752, 2010.

[22] J. Winkler, L. Duenas-Osorio, R. Stein, and D. Subramanian, "Performance assessment of topologically diverse power systems subjected to hurricane events," *Rel. Eng. Syst. Saf.*, vol. 95, no. 4, pp. 323–336, 2010.

[23] S. D. Guikema, R. Nateghi, S. M. Quiring, A. Staid, A. C. Reilly, and M. Gao, "Predicting hurricane power outages to support storm response planning," *IEEE Access*, vol. 2, pp. 1364–1373, 2014.

[24] Y. Wang, C. Chen, J. Wang, and R. Baldick, "Research on resilience of power systems under natural disasters—A review," *IEEE Trans. Power Syst.*, vol. 31, no. 2, pp. 1604–1613, Mar. 2016.

[25] A. Arab, E. Tekin, A. Khodaei, S. K. Khator, and Z. Han, "System hardening and condition-based maintenance for electric power infrastructure under hurricane effects," *IEEE Trans. Rel.*, vol. 65, no. 3, pp. 1457–1470, Sep. 2016.

[26] E. Byon, L. Ntaimo, and Y. Ding, "Optimal maintenance strategies for wind turbine systems under stochastic weather conditions," *IEEE Trans. Rel.*, vol. 59, no. e2, pp. 393–404, Jun. 2010.

[27] A. Arab, A. Khodaei, Z. Han, and S. K. Khator, "Proactive recovery of electric power assets for resiliency enhancement," *IEEE Access*, vol. 3, pp. 99–109, 2015.

[28] A. Arab, A. Khodaei, S. K. Khator, K. Ding, V. A. Emesih, and Z. Han, "Stochastic pre-hurricane restoration planning for electric power systems infrastructure," *IEEE Trans. Smart Grid*, vol. 6, no. 2, pp. 1046–1054, Mar. 2015.

[29] P. Van Hentenryck and C. Coffrin, "Transmission system repair and restoration," *Math. Program.*, vol. 151, no. 1, pp. 347–373, 2015.

[30] C. Coffrin and P. Van Hentenryck, "Transmission system restoration with co-optimization of repairs, load pickups, and generation dispatch," *Int. J. Elect. Power Energy Syst.*, vol. 72, pp. 144–154, 2015.

[31] A. Golshani, W. Sun, Q. Zhou, Q. P. Zheng, and J. Tong, "Two-stage adaptive restoration decision support system for a self-healing power grid," *IEEE Trans. Ind. Inform.*, vol. 13, no. 6, pp. 2802–2812, Dec. 2017.

[32] Y. Fang, N. Pedroni, and E. Zio, "Resilience-based component importance measures for critical infrastructure network systems," *IEEE Trans. Rel.*, vol. 65, no. 2, pp. 502–512, Jun. 2016.

[33] C. M. Rocco, J. E. Ramirez-Marquez, D. E. Salazar, and C. Yajure, "Assessing the vulnerability of a power system through a multiple objective contingency screening approach," *IEEE Trans. Rel.*, vol. 60, no. 2, pp. 394–403, Jun. 2011.

[34] C. Wang, Y. Hou, F. Qiu, S. Lei, and K. Liu, "Resilience enhancement with sequentially proactive operation strategies," *IEEE Trans. Power Syst.*, vol. 32, no. 4, pp. 2847–2857, Jul. 2017.

[35] N. Yodo, P. Wang, and Z. Zhou, "Predictive resilience analysis of complex systems using dynamic Bayesian networks," *IEEE Trans. Rel.*, vol. 66, no. 3, pp. 761–770, Sep. 2017.

[36] M. Sahraei-Ardakani and G. Ou, "Day-ahead preventive scheduling of power systems during natural hazards via stochastic optimization," in *Proc. IEEE Power Energy Soc. Gen. Meeting*, Chicago, IL, USA, 2017, pp. 1–5.

[37] Y. Sang, M. Sahraei-Ardakani, J. Xue, and G. Ou, "Effective scenario selection for preventive stochastic unit commitment during hurricanes," in *Proc. IEEE Int. Conf. Probab. Methods Appl. Power Syst.*, 2018, pp. 1–6.

[38] Y. Sang, J. Xue, M. Sahraei-Ardakani, and G. Ou, "Comparing a new power system preventive operation method with a conventional industry practice during hurricanes," in *Proc. 51st North Amer. Power Symp.*, Wichita, KS, USA, Oct. 2019, pp. 1–6.

[39] E. D. Vugrin, A. R. Castillo, and C. A. Silva-Monroy, "Resilience metrics for the electric power System: A performance-based approach," Sandia Nat. Lab., Albuquerque, NM, USA, Tech. Rep. SAND2017-1493, 2017.

[40] A. Veeramany *et al.*, "Framework for modeling high-impact, low-frequency power grid events to support risk-informed decisions," Pacific Northwest Nat. Lab., Richland, WA, USA, Tech. Rep. PNNL-24673, 2015.

[41] *2017 National Electrical Safety Code(R) (NESC(R))*, pp. 1–405, Aug. 2016.

[42] "New York state transmission and distribution systems reliability study and report," New York State Energy Planning Board, Albany, NY. 2012. [Online]. Available: http://nyssmartgrid.com/wp-content/uploads/2012/09/reliability-study.pdf

[43] "*Florida Power and Light News Releases*, Florida Power Light Company: FPL Newsroom, 2017. [Online]. Available: http://newsroom.fpl.com/2017-09-07-FPL-mobilizes-restoration-workforce-of-more-than-11-000-employees-and-contractors-as-it-prepares-for-potential-landfall-of-Hurricane-Irma, Accessed: Nov. 18, 2018

[44] "Build Back Better: Reimagining and strengthening the power Grid of Puerto Rico," Res. Rep., Dec. 2017. [Online]. Available: https://sepapower.org/resource/build-back-better-reimagining-and-strengthening-the-power-grid-of-puerto-rico

[45] "Energy resilience solutions for the Puerto Rico Grid," US Dept. Energy, Washington, DC, USA, Tech. Rep., Jun. 2018. [Online]. Available: https://www.energy.gov/sites/prod/files/2018/06/f53/DOE%20Report_Energy%20Resilience%20Solutions%20for%20the%20PR%20Grid%20Final%20June%202018.pdf
[46] K. LaCommare, P. Larsen, and J. Eto, "Evaluating proposed investments in power system reliability and resilience: preliminary results from interviews with public utility commission staff," Lawrence Berkeley Nat. Lab., Berkeley, CA, USA, Tech. Rep. LBNL-1006971, Jan. 2017.
[47] A. Forbes, "Lessons learned: How utilities have prepared for hurricane season," Gen. Elect., Boston, MA, USA, Jun. 2018.
[48] *A Stronger, More Resilient New York–Chapter 6: Utilities*, New York, NY, USA, Jun. 2013. [Online]. Available: https://www1.nyc.gov/assets/sirr/downloads/pdf/Ch_6_Utilities_FINAL_singles.pdf
[49] P. Hoffman, W. Bryan, and A. Lippert, "Comparing the Impacts of the 2005 and 2008 hurricanes on US energy infrastructure," US Dept. Energy, Washington, DC, USA, 2009.
[50] P. A. Hirschberg *et al.*, "A weather and climate enterprise strategic implementation plan for generating and communicating forecast uncertainty information," *Bull. Amer. Meteorol. Soc.*, vol. 92, no. 12, pp. 1651–1666, Aug. 2011.
[51] B. Asgarian, S. Dadras Eslamlou, A. E. Zaghi, and M. Mehr, "Progressive collapse analysis of power transmission towers," *J. Constructional Steel Res.*, vol. 123, no. Suppl. C, pp. 31–40, Aug. 2016.
[52] H. Yasui, H. Marukawa, Y. Momomura, and T. Ohkuma, "Analytical study on wind-induced vibration of power transmission towers," *J. Wind Eng. Ind. Aerodyn.*, vol. 83, no. 1, pp. 431–441, 1999.
[53] J. D. Holmes, *Wind Loading of Structures*, 3rd ed. Boca Raton, FL, USA: CRC Press, 2017.
[54] A. G. Davenport, "The spectrum of horizontal gustiness near the ground in high winds," *Quart. J. Roy. Meteorological Soc.*, vol. 87, no. 372, pp. 194–211, 1961.
[55] T. Mara, "Capacity assessment of a transmission tower under wind loading," Ph.D. Diss., Dept. Civil Environ. Eng., The Univ. Western Ontario, London, ON, Canada, Aug. 2013.
[56] M. Shinozuka and C.-M. Jan, "Digital simulation of random processes and its applications," *J. Sound Vib.*, vol. 25, no. 1, pp. 111–128, Nov. 1972.
[57] B. R. Ellingwood, "Earthquake risk assessment of building structures," *Rel. Eng. Syst. Saf.*, vol. 74, no. 3, pp. 251–262, 2001.
[58] G. J. Holland, "An analytic model of the wind and pressure profiles in hurricanes," *Monthly Weather Rev.*, vol. 108, no. 8, pp. 1212–1218, 1980.
[59] Univ. Washington, Seattle, WA, USA, Power Systems Test Case Archive: IEEE 118-Bus Test System, 1993. [Online]. Available: https://labs.ece.uw.edu/pstca/pf118/pg_tca118bus.htm
[60] National Hurricane Center, Miami, FL, USA. Accessed: Jan. 4, 2018. [Online]. Available: http://www.nhc.noaa.gov/
[61] Y. Sang and M. Sahraei-Ardakani, "The interdependence between transmission switching and Variable-Impedance series FACTS devices," *IEEE Trans. Power Syst.*, vol. 33, no. 3, pp. 2792–2803, May 2018.

Yuanrui Sang (S'14–M'20) received the Ph.D. degree in electrical and computer engineering from The University of Utah, Salt Lake City, UT, USA, in 2019.

She is currently an Assistant Professor with the Department of Electrical and Computer Engineering, The University of Texas at El Paso, El Paso, TX, USA. Her research interests include power system resilience, power system economics, and flexible transmission systems.

Jiayue Xue received the M.S. degree in structural engineering from the University of Michigan, Ann Arbor, MI, USA, in 2014. She is currently working toward the Ph.D. degree with the Department of Civil and Environmental Engineering, The University of Utah, Salt Lake City, UT, USA.

Her research interests include regional hazard analysis, power system vulnerability analysis, and wind fragility analysis.

Mostafa Sahraei-Ardakani (M'06) received the Ph.D. degree in energy engineering from The Pennsylvania State University, University Park, PA, USA, in 2013.

He is currently an Assistant Professor with the Department of Electrical and Computer Engineering, The University of Utah, Salt Lake City, UT, USA. Prior to his current position, he was a Postdoctoral Research Scholar with Arizona State University, Tempe, AZ, USA. His research interests include energy economics and policy, electricity markets, power system optimization, power system resilience, and interdependent infrastructure systems.

Ge (Gaby) Ou received the B.Sc. degree in theoretical and applied mechanics from the Harbin Institute of Technology, Harbin, China, the B.E. degree in civil engineering from The University of Sydney, Sydney, NSW, Australia, in 2010, and the Ph.D. degree in structural engineering from Purdue University, West Lafayette, IN, USA, in 2016.

In 2016, she joined the Department of Civil and Environmental Engineering, The University of Utah, as an Assistant Professor. Her research interests lie in the areas of regional hazard analysis and mitigation, advanced experimental and computational structural analysis, and structural damage assessment and monitoring.